

# Dynamic Random Access Memory Based on Fiber Optic Lines for Optical Computers. Computer Modeling

Andriy Semenov <sup>1</sup>, Serhii Tsyruynyk <sup>2,3</sup>, Olena Semenova <sup>1</sup>, Serhii Baraban <sup>4</sup> and Anton Khloba <sup>1</sup>

<sup>1</sup> Vinnytsia National Technical University, Khmelnytske highway, 95, Vinnytsia, 21021, Ukraine

<sup>2</sup> Vinnytsia Technical College, Khmelnytske highway, 91/2, Vinnytsia, 21021, Ukraine

<sup>3</sup> Vinnytsia National Agrarian University, str. Sonyachna, 3, Vinnytsia, 21008, Ukraine

<sup>4</sup> Poznan University of Technology, plac Marii Skłodowskiej-Curie 5, Poznan, 60965, Poland

## Abstract

The study proposes the structure of construction and technical implementation of an optical operational storage device based on fiber-optic lines for optical computers. The basic element is a ring-type storage device on fiber-optic lines, in which information circulates as a wave packet of optical pulses along a closed fiber circuit. The operating range of 1550 nm is used to reduce optical losses. Using NZDSF fiber of the SMF-LS type is justified to compensate for the polarisation mode dispersion. An SOA amplifier is used to restore the optical signal level. An electro-optical directional splitter is used to input/output optical signals. To work with optoelectronic memory on fiber-optic lines, it is recommended to use a femtosecond fiber laser and the wave-coding method. The study found that using fiber-optic lines can increase the speed of information flow up to ten times by reducing the time spent on the RAM operation.

## Keywords

Optical RAM, NZDSF type SMF-LS, SOA amplifier, mode dispersion compensation, wave coding.

## 1. Introduction

The appearance of optical fibers with low losses and a large product of length by bandwidth is opening up prospects in optical signal processing. It becomes possible to create fiber-optic devices when performing operations such as convolution, calculation of correlation functions, matrix operations, filtering, pulse generation, code combinations, pulse compression, and matched filtering [1, 2].

However, the dynamic storage of light pulses for optical computers and optical information transmission systems is very relevant. Potentially, a light beam can have a spectral width comparable to its carrier frequency, i.e., can be of the order of  $10^{-13} \sim 10^{-14}$  seconds. Paper [3] considers the basic element of an optical dynamic operational storage device that can store both analog and digital optical information. The basic element is a ring-type storage device on a fiber-optic line, in which information circulates in the form of a burst of optical pulses along a closed fiber circuit [4].

Paper [5] presents the results of a study of n-bit optical dynamic RAM. The cells of this optical dynamic RAM have arbitrary access for writing, reading, and updating operations during optical computing. In the proposed RAM [5], the authors implemented a 1-bit memory element based on a semiconductor optical amplifier with random asynchronous access. Also, [5] presents the study results of this 1-bit memory element. In [6], the authors proposed the structure of an optoelectronic dynamic RAM. Optical information is stored in the memory element using a fiber-optic delay line. This made it possible to develop a high-speed buffer memory without losing optical information [6]. In [7], a structure of n-bit optical dynamic RAM was proposed, which

---

COLINS-2024: 8th International Conference on Computational Linguistics and Intelligent Systems, April 12–13, 2024, Lviv, Ukraine

✉ semenov.a.o@vntu.edu.ua (A. Semenov); sovmsvom@gmail.com (S. Tsyruynyk); semenova.o.o@vntu.edu.ua (O. Semenova); serhii.baraban@put.poznan.pl (S. Baraban); hlobaanton@gmail.com (A. Khloba)

ORCID: 0000-0001-9580-6602 (A. Semenov); 0000-0002-5703-9761 (S. Tsyruynyk); 0000-0001-5312-9148 (O. Semenova); 0000-0001-9535-1644 (S. Baraban); 0009-0007-6743-2456 (A. Khloba)



© 2024 Copyright for this paper by its authors.

Use permitted under Creative Commons License Attribution 4.0 International (CC BY 4.0).

consists of a matrix of 1-bit optical dynamic RAM elements. The single-bit cells of the optical dynamic RAM are built based on a semiconductor optical amplifier using a fiber optic loop [7].

All the variants of optical dynamic RAM proposed in publications [3-7] have a limited speed of about 10 Gbit/s. The aim of this work is a model study of the physical parameters and characteristics of a variant of the implementation of a dynamic optical random access memory device based on fiber-optic lines for optical computers with a speed of more than 10 Gbit/s.

## 2. Models and Methods

The block diagram of the basic element of the dynamic optical operational storage device (DOOSD) on fiber-optic lines (FOLs), shown in Figure 1, allows you to input an optical signal either through  $U_{bx1}$  or  $U_{bx2}$ . Similarly, the information can be read out either through  $U_{bux1}$  or  $U_{bux2}$ .

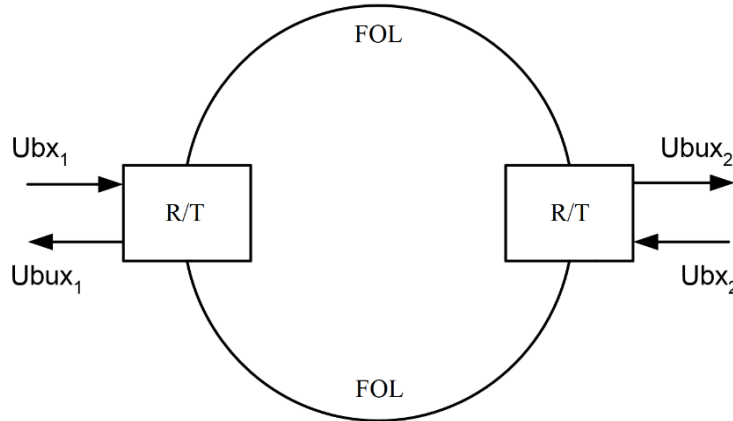


**Figure 1:** Block diagram of the basic element DOOSD

According to [8], the polarization mode dispersion coefficient for NZDSF fiber of SMF-LS type is equal to  $T = 0.5 \text{ ps} / \sqrt{\text{km}}$ , and the chromatic dispersion coefficient  $D = 3.5 / \text{nm} \cdot \text{km}$ . Considering the presence of two electro-optical switches, the polarization mode dispersion coefficient should be increased to 1. The polarization mode dispersion is determined from the formula [9]:

$$\tau_{pmd} = T \cdot \sqrt{L}. \quad (1)$$

The distance  $L$  at which the chromatic and polarization dispersion become equal:

$$L_0 = \left( \frac{T}{D(\lambda)\Delta\lambda} \right)^2 = \left( \frac{1}{3.5 \cdot 0.05} \right)^2 = 32.65 \text{ cm}. \quad (2)$$

Liouville's theorem [10, 11] shows that single-mode fiber optic fibers are compatible with single-mode planar, channel, and strip optical fibers in an integrated design. Paper [12] discusses the peculiarities of the transition of homogeneous media to a wafer (silicon substrate with a diameter of 300~400 mm), which allows the implementation of optical computing systems for various purposes on their basis. The dimensions of the wafer actually determine the size of the optical fiber ring [13]. If we assume the length of the optical fiber optic ring of the basic element of the DOOSD to be 32.65 cm, the ring diameter is equal to:

$$D = \frac{L}{\pi} = \frac{32.65}{3.14} = 10.4 \text{ cm}. \quad (3)$$

The selected size of the optical fiber ring allows it and additional elements (electro-optical switches) to be placed on the wafer. Thus, the optical pulse must make 100000 revolutions to cover a distance of 32.65 cm.

Let's calculate the attenuation of the optical signal in the basic element of the DOOSP. The signal attenuation depends on the signal attenuation in the optical fiber, the signal loss introduced by the electro-optical switch, and the bending loss of the fiber. According to [14], bending losses can be neglected if the bending radius is of the order of 10 mm, which is the case (the bending radius of the optical fiber ring is 52 mm). The signal attenuation in an optical fiber is equal to:

$$\alpha_{fib} = K_{\alpha} \cdot L_0 = 0.25 \cdot 32.65 = 8.16 \text{ dB} , \quad (4)$$

where  $K_{\alpha}$  is the maximum attenuation of the SMF-LS fiber [8];  $L_0$  is the distance at which the chromatic and polarization dispersion is equal to each other.

According to [4], the loss of an electro-optical switch is 4 dB, and since two of them are required (Figure 1), the total loss from electro-optical switches is 8 dB. Thus, the total loss is equal to:

$$\alpha = 8.16 + 8.0 = 16.16 \text{ dB} . \quad (5)$$

The wave coding method is used to encode the information sequence and store it in the DOOSP. The frequency plan of WDM systems provides for 37 nominal central wavelengths for 100 GHz increments in the range 1538.77 nm...1560.61 nm, so there are no complications with the choice of wavelengths  $\lambda_1$  and  $\lambda_2$  [15].

Femtosecond fiber lasers can generate pulses with tens of tens of femtoseconds to 5~6 fs, which implies stable and steady operation without needing constant system adjustment. The low cost and stability of femtosecond fiber lasers make it possible to use them to generate an information sequence of optical pulses for the DOOSD [16].

The information capacity is equal to the number of pulses with a duration of 100 fs that can be placed in the time  $T$  that a light pulse will travel through an optical ring of 32.65 cm in length:

$$T = \frac{L}{c} = \frac{0.3265}{3 \cdot 10^8} = 1.088 \cdot 10^{-9} \text{ s} , \quad (6)$$

$$I = \frac{T}{t_i} = \frac{1.088 \cdot 10^{-9}}{0.1 \cdot 10^{-12}} = 10.88 \cdot 10^3 \approx 10 \text{ Kbit} . \quad (7)$$

The storage time can be defined as the time for a light pulse to travel a distance  $L_0$ :

$$t_{st} = \frac{L_0}{c} = 1.088 \cdot 10^{-4} \text{ s} \approx 100 \text{ ms} . \quad (8)$$

The duration of the read and write cycle is determined by the length of the optical fiber ring and is equal to  $T$ :

$$t_R = t_W = T = 1.088 \cdot 10^{-9} \text{ s} . \quad (9)$$

The speed of the electro-optical switch determines the access time at the first access (Latency) and is equal to  $t_L = 10 \text{ ps}$ . The maximum data throughput (baud rate) is defined as the ratio of the number of pulses located in the optical fiber ring with a length of 32.65 cm to the time of their passage through the ring:

$$BW = \frac{l}{T} = \frac{10 \cdot 10^3}{1 \cdot 10^{-9}} = 10 \text{ Tbit} / \text{s} . \quad (10)$$

The parameters of the basic element of the DOOSD are given in Table 1.

**Table 1**  
**Limit operating parameters of the basic element of the DOOSD**

Parameter	Unit of measurement	Value
Information capacity	Kbit	10
Organization		10Kbit×1
Information storage time	μs	100
Read cycle time	ns	1
Write cycle time	ns	1
Access time at the first access	ps	10
Transmission rate	Tbit/s	10
Signal attenuation	dB	16
The wavelength of the optical signal	nm	1560 ± 10
Optical power of the input signal	mW	<10

When optical pulses pass through the FOC, nonlinear phenomena occur: stimulated Brillouin scattering (SBS), stimulated Raman scattering (SRS), self-phase modulation (SPM), quarter-wave shift, etc. [8]. Nonlinear interaction between the optical signal and the optical fiber transmission medium occurs when the optical signal power is increased. To preserve the optical pulses, it is necessary to use the linear mode of optical pulse propagation in the fiber. At the optical signal power  $P_{in} < 10 \text{ mW}$ , the nonlinear interaction between the optical signal and the optical fiber does not occur.

As the pulses circulate along the circuit, the shape, amplitude, and position of the pulses change [17]. To reduce optical losses, the operating range of 1550 nm is used in the DOOSD, and to compensate for polarization mode dispersion, NZDSF fiber of SMF-LS type is used; however, according to calculations (Table 1), the pulse amplitude is reduced by 16 dB. Therefore, in order to restore or further use the optical information sequence, it must be restored (regenerated). For this purpose, an optical amplifier with a gain of 16 dB should be used, which introduces as little noise as possible and allows it to be made in an integrated design for combining in one housing with the DOOSD cell.

Semiconductor optical amplifiers are small in size and weight [18]; they use direct conversion of electrical energy into optical energy, which results in significantly lower power consumption [19]; they are cheaper and have come close to fiber optic amplifiers in terms of their technical characteristics [20]. The amplifying medium in SOA is a semiconductor structure made of (GaAl)As crystal with geometric dimensions of no more than a few millimeters, which makes it possible to integrate such amplifiers together with other elements of integrated circuits, for example, with the basic element of a DOOSD [21].

In [22], the description and main characteristics of the SOA amplifier for the range of 1530...1560 nm are given. It can be used as an optical signal amplifier to restore its level after storage in the DOOSD.

### 3. Results and Discussion

Computer modeling aims to confirm the possibility of implementing the DOOSD on FOCL [5]. The software package Synopsys OptSim for Optical Communication, which is a CAD program for modeling fiber-optic systems, was used for the research. In the course of the research, the following tasks were set:

- Determination of the optical signal loss with a wavelength of 1.55 μm when passing through the NZDSF fiber of SMF-LS type at a distance of 33~35 km;
- Determination of the influence of polarization mode dispersion on the waveform and the possibility of its compensation;

- Determination of the optical input power value at which the linear mode of signal transmission in the FOCL is ensured.

As a result of the experimental studies, the following results were obtained. Figure 2 shows a PRBS generator that forms a digital information sequence, an NRZ transmitter, an optical filter, an attenuator, a receiver, a BER tester, a spectrum analyzer, and an oscilloscope. The NRZ transmitter consists of a CW laser, an electric generator (NRZ driver), an external Mach-Zehnder modulator, and an attenuator. The waveform and spectrum of the signal input to the fiber are shown in Figure 3.

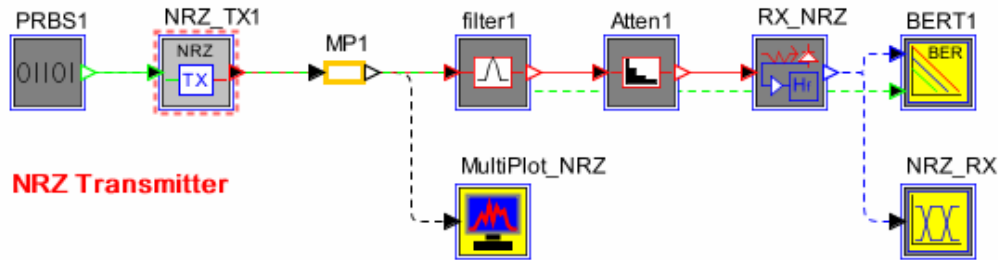


**Figure 2:** Structure-function diagram of the optical information sequence source shape study

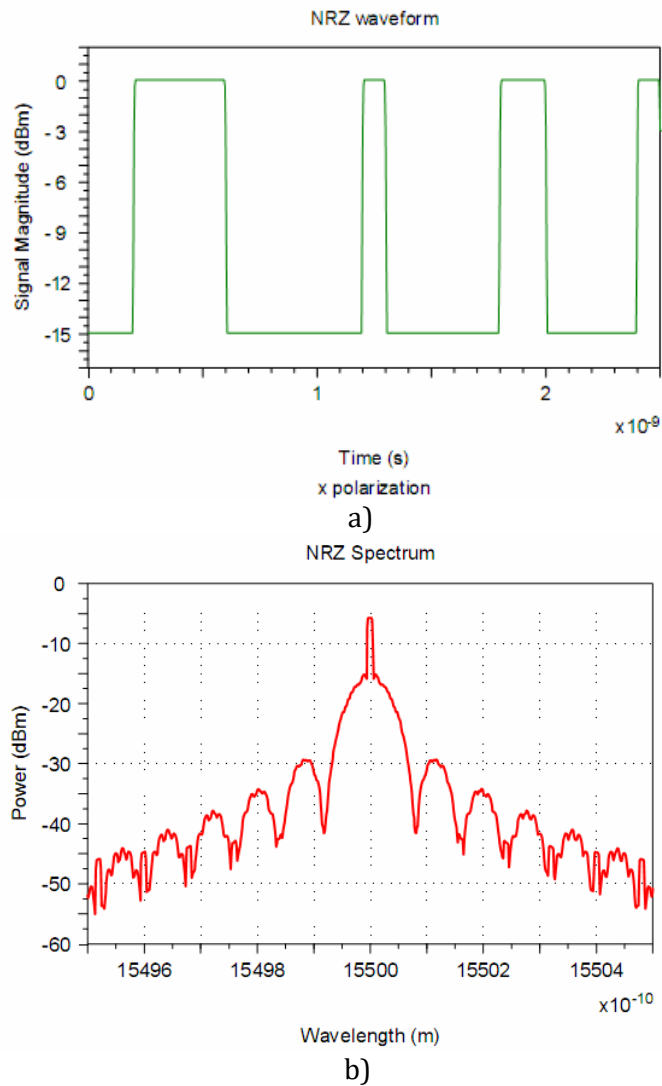


**Figure 3:** Waveform a); spectrum b) of the transmitter signal

At the output of the optical signal receiver (RX\_NRZ), we observe the picture (Figure 4). To measure the losses during the passage of an optical information sequence (see Figure 3) through a 35 km long NZDSF fiber, the scheme shown in Figure 5 is used.

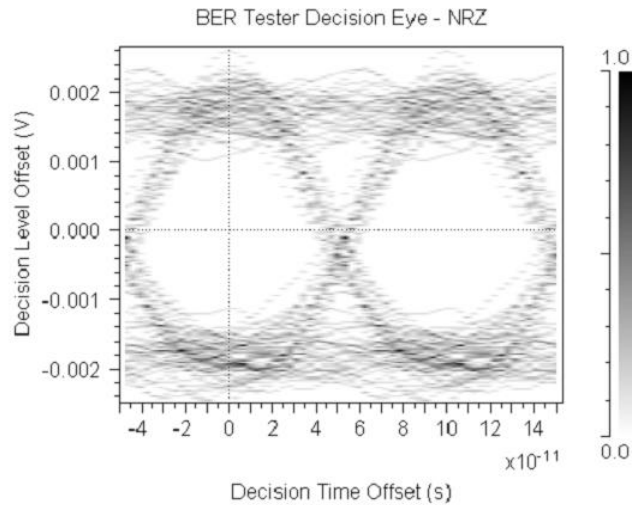


**Figure 4:** Eye diagram at the output of the optical signal receiver

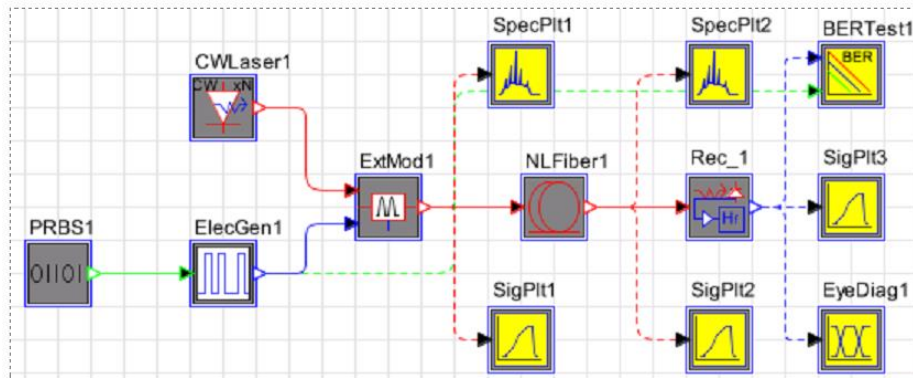


**Figure 5:** Scheme for the study of losses in the fiber

Figure 6 and Figure 7 show the waveforms of the transmitter and receiver respectively (the effect of polarization is not considered). Figure 6 and Figure 7 shows that the optical signal loss equals  $D = 4.75 - (-3.8) = 8.55 \text{ dB}$ , corresponding to the parameters (Table 1).

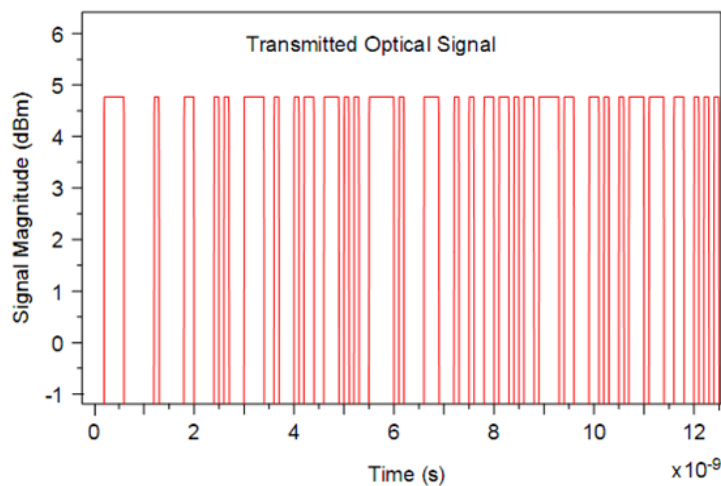


**Figure 6:** The transmitted optical signal

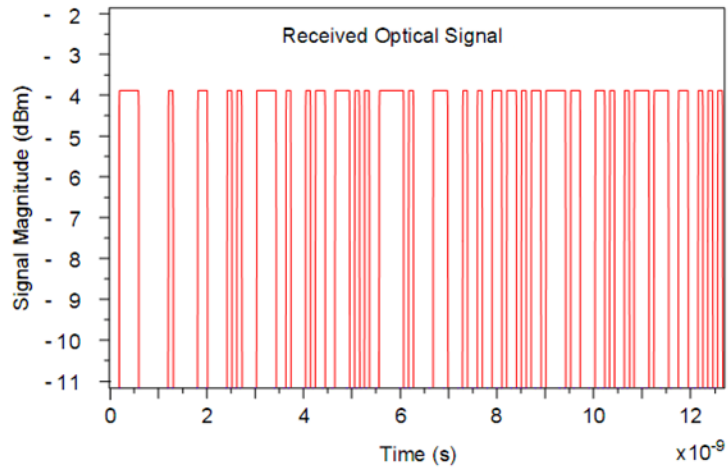


**Figure 7:** The received optical signal (the length of the fiber is 35 km)

Accordingly, the eye diagram will look like the one shown in Figure 8. The effect of polarization mode dispersion is studied according to the scheme shown in Figure 9. The fiber length is chosen to be 33 km; the PMD polarization coefficient is  $1.0 \text{ ps} / \text{km}^{1/2}$ .

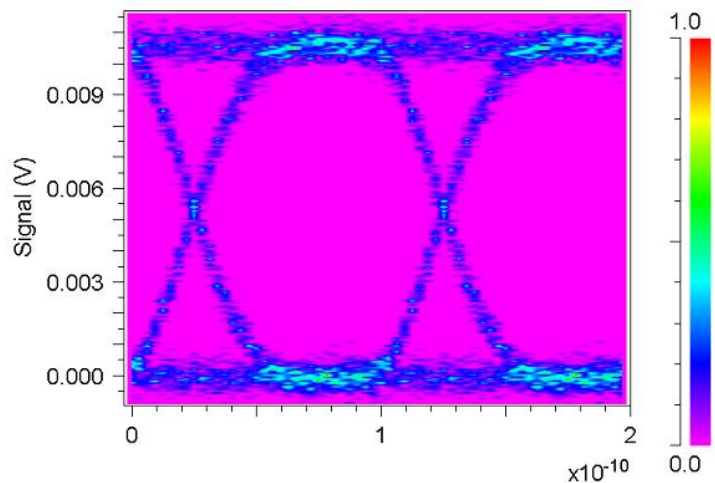


**Figure 8:** Eye diagram of the received signal

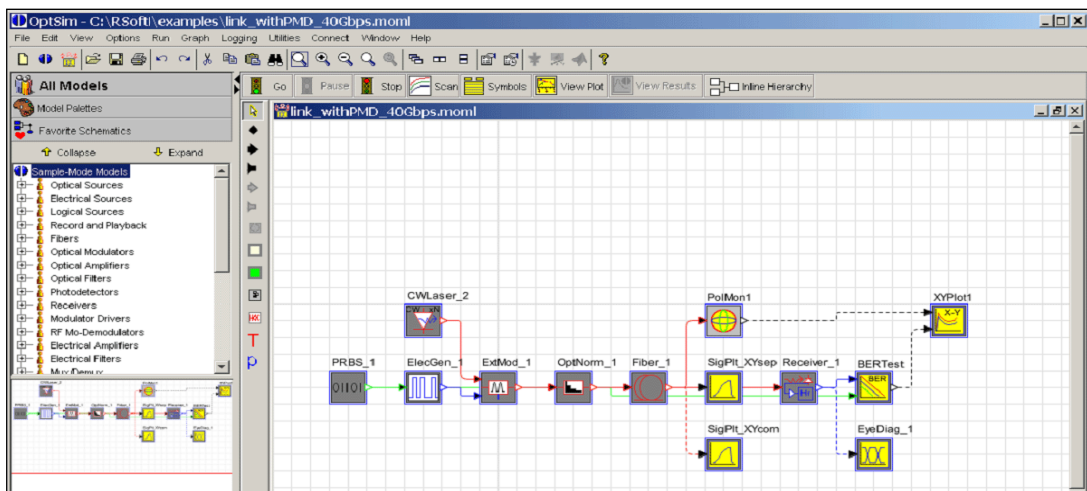
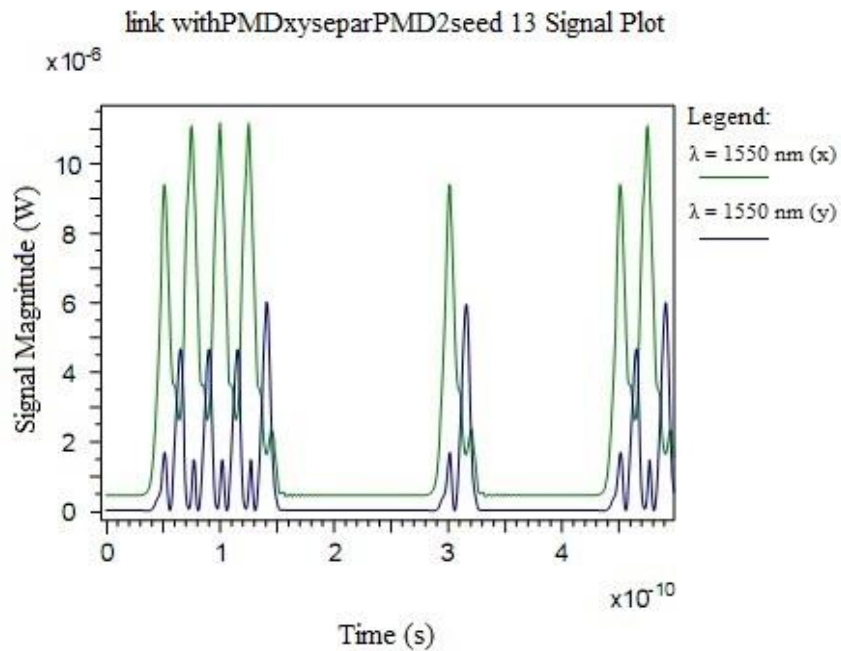
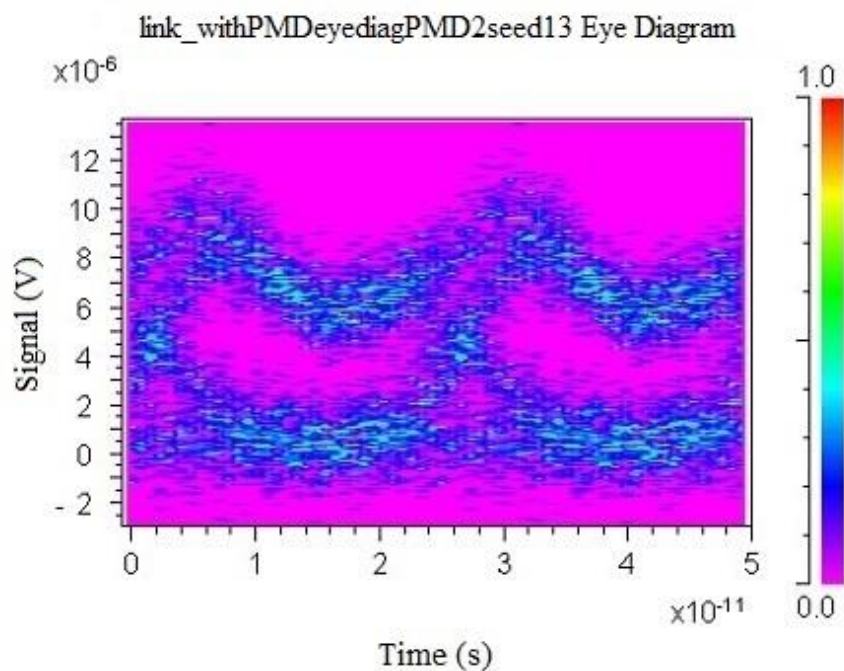


**Figure 9:** OPTSIM software window with a diagram for studying the effect of polarization mode dispersion on the optical signal shape when passing through DSF, NZDSF fiber

The signal characteristics are shown in Figure 10. Figure 11 shows that the NZDSF fiber of SMF-LS type with a negative chromatic dispersion compensates for the effect of polarization mode dispersion at a distance of 33-35 km, which can be used to build a DOOSD on the FOCL. To study the power level to be input to the DOOSD, we use the scheme shown in Figure 12.



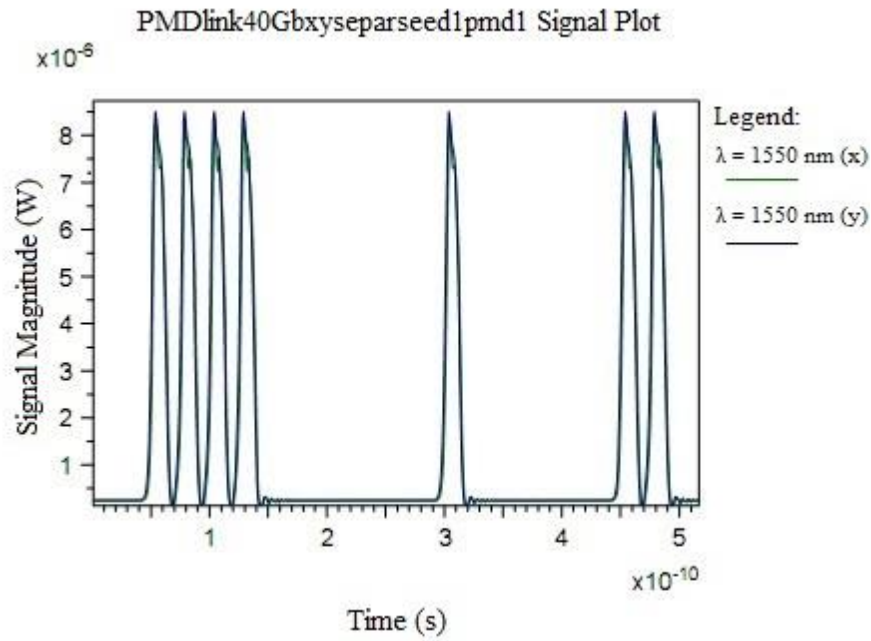
a)



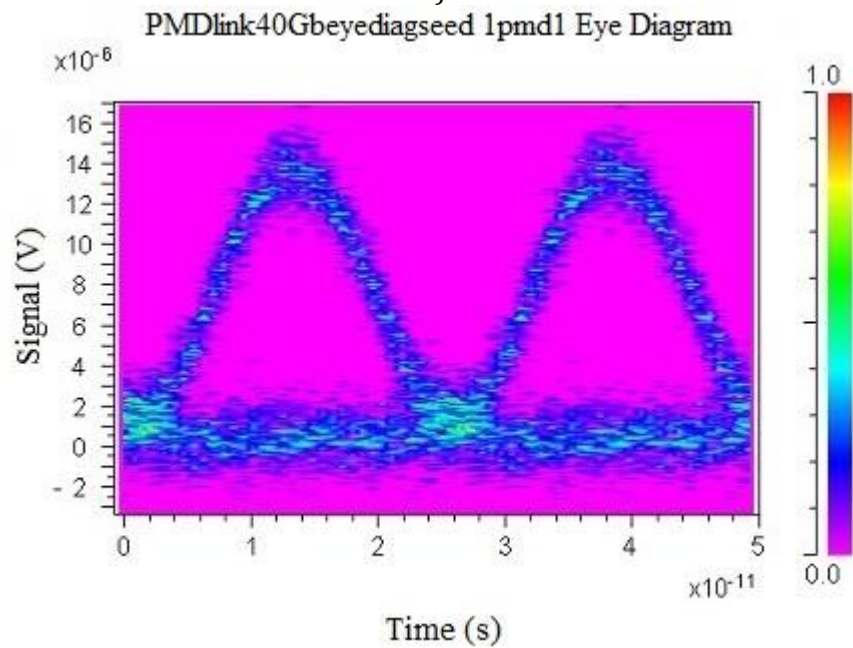
b)

**Figure 10:** The result of the effect of polarization mode dispersion on signal propagation in DSF fiber, oscillogram of the signal at the fiber output a); eye diagram of the photodetector b)

For the linear mode of operation of the FOCs, it was recommended to use an input optical power of less than 10 mW [5]. The tests were carried out twice: at 10 mW, the modulator output was 10 dB, and at 50 mW, 17.5 dB. The initial parameters of the signal source are shown in Figure 13.



a)



b)

**Figure 11:** The result of the effect of polarization mode dispersion on signal propagation in NZDSF (SMF-LS) fiber, waveform of the signal at the fiber output a); eye diagram of the photodetector b)

Figures 14 and 15 show that at an input power of more than 10 mW, a nonlinear mode of operation occurs in the fiber, which leads to distortion of the information stored in the DUT. Therefore, the input power of the optical information sequence input to the storage device should be less than 10 mW.

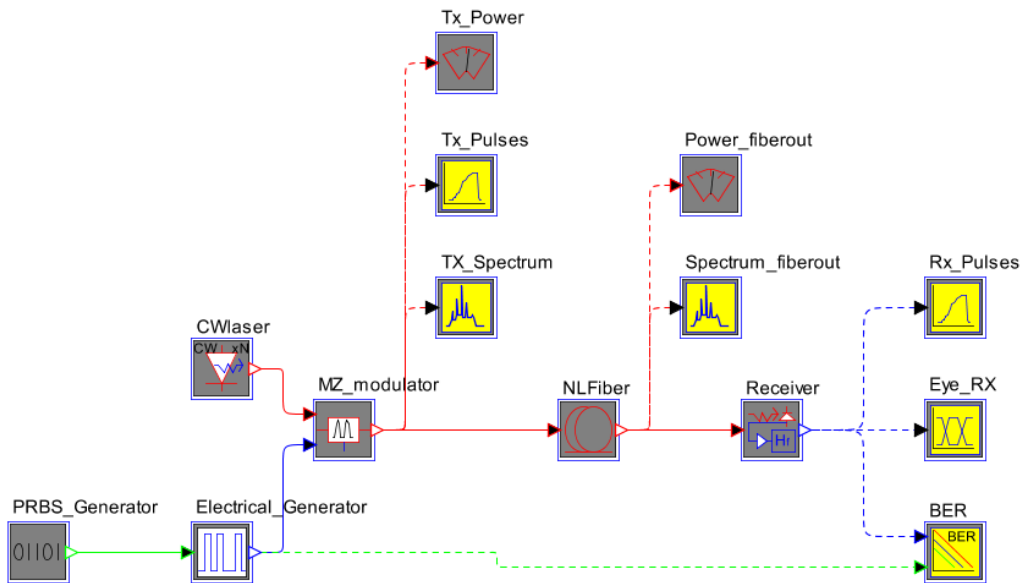


**Figure 12:** Scheme for studying the level of optical power to be introduced into the fiber

Properties for CWlaser

Help From Disk... Load ... Save ...

Optical Ports Naming

Parameter	Value	Units	Range	Std. Dev.	Distribution
peakPower	10.0	mW	[0, 1e+018]	0.0	None
wavelength	1550e-9	meters	[0, 1e+018]	0.0	None
mode	"Single"				
multiNodeOutput	"NO"				
noSources	10	none	[1, 1000]		
deltaFreq	100e9	meters or Hz	[0, 1e+018]	0.0	None
filename	""				
azimuth	0.0	degrees	[-90, 90]	0.0	None
ellipticity	0.0	degrees	[-45, 45]	0.0	None

**Figure 13:** CWlaser parameters before starting the test

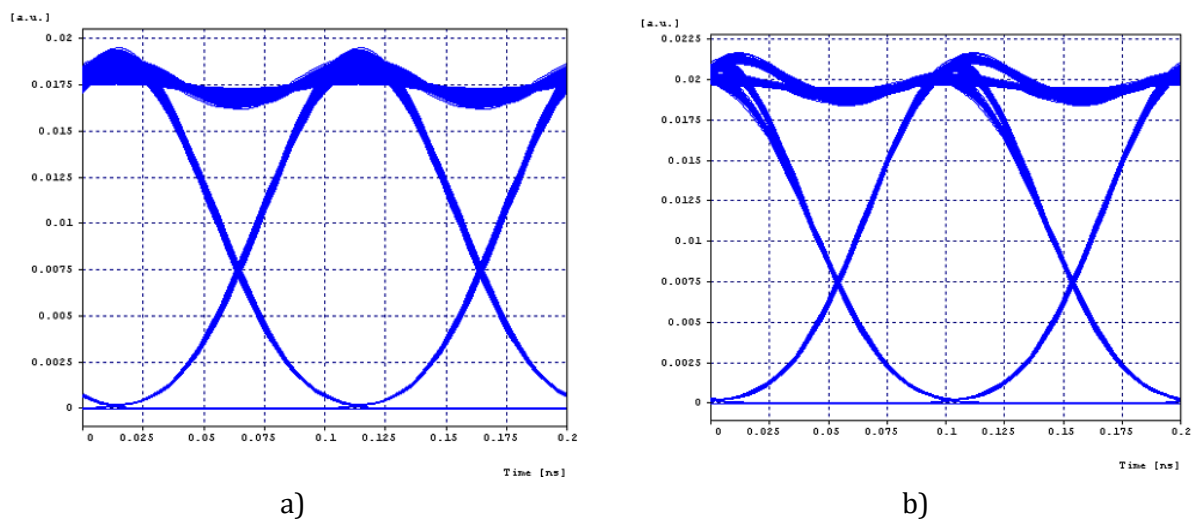


**Figure 14:** Eye diagram at a signal source power of 10 mW (10 dB) at the fiber input a); at the fiber output b)

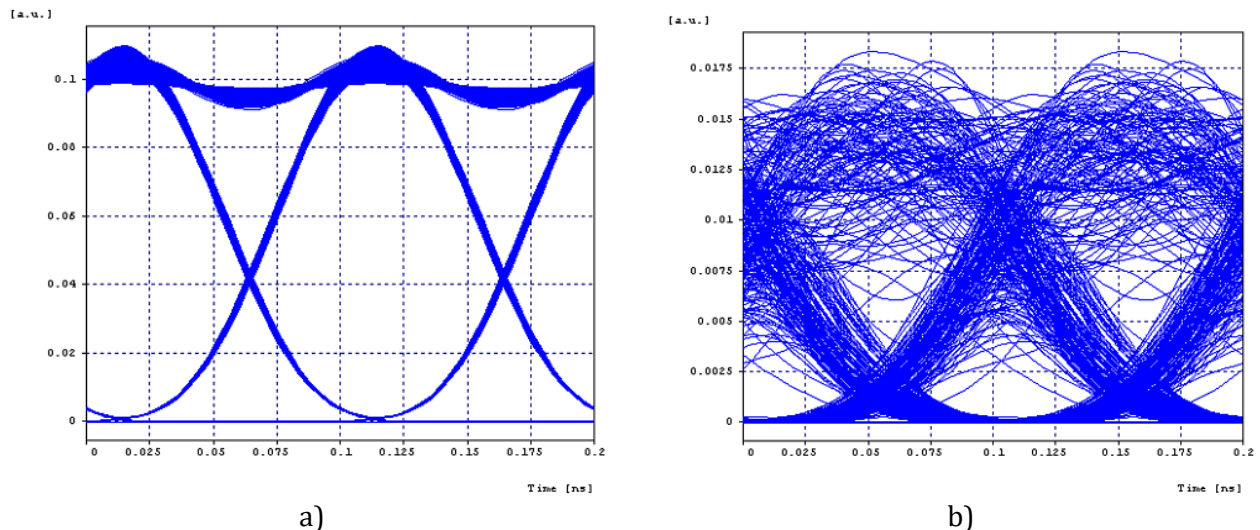


**Figure 15:** Eye diagram at a signal source power of 50 mW (17.5 dB) at the fiber input a); at the fiber output b)

## 4. Conclusions

The results of computer modeling confirmed the possibility of implementing a dynamic random access optical storage device based on fiber-optic lines for optical computers. To reduce optical losses in a dynamic optical random access memory, it is advisable to use the operating range of 1550 nm. To compensate for PMD, NZDSF type SMF-LS should be used. An SOA amplifier can be used to restore the optical signal level. Optical signals are input/output through an electro-optical directional coupler. To work with optoelectronic memory on fiber optic lines, it is recommended to use a femtosecond fiber laser and the wave coding method. In further research, the authors will develop an experimental model of a dynamic optical random access storage device based on fiber optic lines for optical computers. The authors will perform experimental studies. The authors will compare the results of experimental studies with the results of computer modeling and draw conclusions about the prospects of the proposed dynamic optical random access storage device based on fiber optic lines for optical computers.

## References

- [1] A. V. Pankov, I. D. Vatnik, A. A. Sukhorukov, Optical Neural Network Based on Synthetic Nonlinear Photonic Lattices, *Physical Review Applied* 17 (2022). doi:10.1103/physrevapplied.17.024011.
- [2] M. Mohseni, A. H. Novin, OML-PCM: optical multi-level phase change memory architecture for embedded computing systems, *Engineering Research Express*, 5 (2023). doi:10.1088/2631-8695/ad0fc4.
- [3] R. Gherabli, R. Zektzer, M. Grajower, J. Shappir, C. Frydendahl, U. Levy, CMOS-compatible electro-optical SRAM cavity device based on negative differential resistance, *Science Advances*, 9 (2023). doi:10.1126/sciadv.adf5589.
- [4] A. R. Yuvaraj, Md. L. Rahman, M. Mohd Yusoff, Synthesis and Light Induced Characteristics of Siloxane Substituted Azobenzene: An Application for Optical Storage Device, *International Journal of Spectroscopy*, 2016 (2016) 1–9. doi:10.1155/2016/4715230.
- [5] G. Berrettini, L. Potì, A. Bogoni, Optical Dynamic Random Access Memory (ODRAM), In: *Proceedings of the Optical Fiber Communication Conference/National Fiber Optic Engineers Conference 2011*, OSA, 2011. doi:10.1364/nfoec.2011.jwa036.
- [6] I. A. Malevich, A. V. Polyakov, S. I. Chubarov, Multichannel fiber optic recirculating memory, In: *Proceedings of the 2011 11th International Conference on Laser and Fiber-Optical*

- Networks Modeling (LFNM), Kharkov, Ukraine, 2011, pp. 1–2, doi: 10.1109/LFNM.2011.6145024.
- [7] G. Berrettini, L. Poti, A. Bogoni, Optical Dynamic RAM for All-Optical Digital Processing, *IEEE Photonics Technology Letters*, 23(11) (2011) 685–687. doi: 10.1109/LPT.2011.2123087.
- [8] Jim Hayes (Ed.), Bee Suat Lim (Preface), *The FOA Reference Guide to Fiber Optic Network Design: Study Guide For FOA Certification*, FOA Reference Textbooks On Fiber Optics Book 7, 2016.
- [9] N. Z. Rashed, K. Krishnan, R. T. Prabu, B. M. Xavier, S. H. Ahammad, Md. A. Hossain, Optical differential phase shift keying transceiver systems performance efficiency at high data rate optical systems in the presence of Pr doped amplifiers, *Journal of Optical Communications*, 0 (2023). doi:10.1515/joc-2023-0025.
- [10] L. Jiang, J. Feng, L. Yan, A. Yi, S.-S. Li, H. Yang, Y. Dong, L. Wang, A. Wang, Y. Wang, W. Pan, B. Luo, Chaotic optical communications at 56 Gbit/s over 100-km fiber transmission based on a chaos generation model driven by long short-term memory networks, *Optics Letters*, 47 (2022) 2382–2385. doi:10.1364/ol.456258.
- [11] G. Rademacher et al., A Comparative Study of Few-Mode Fiber and Coupled-Core Multi-Core Fiber Transmission, *Journal of Lightwave Technology*, 40 (2022) 1590–1596. doi:10.1109/jlt.2021.3124521.
- [12] H. Sui, H. Zhu, J. Wu, B. Luo, S. Taccheo, X. Zou, Modeling pulse propagation in fiber optical parametric amplifier by a long short-term memory network, *Optik*, 260 (2022) 169125. doi:10.1016/j.ijleo.2022.169125.
- [13] H. Mekawey, M. Elsayed, Y. Ismail, M. A. Swillam, Optical Interconnects Finally Seeing the Light in Silicon Photonics: Past the Hype, *Nanomaterials* 12.3 (2022) 485. doi:10.3390/nano12030485.
- [14] A. N. Zaki Rashed, et al., Ideal single mode laser operation with single drive conventional/phase shift Mach-Zehnder modulators measured in optical access networks, *Journal of Optical Communications*, 0 (2022). doi:10.1515/joc-2022-0221.
- [15] E. Buks, Tunable Multimode Lasing in a Fiber Ring, *Physical Review Applied*, 19 (2023) L051001. doi:10.1103/physrevapplied.19.l051001.
- [16] T. Alexoudi, G.T. Kanellos, N. Pleros, Optical RAM and integrated optical memories: a survey, *Light: Science & Applications* 9.1 (2020). doi:10.1038/s41377-020-0325-9.
- [17] A. Semenov, S. Baraban, M. Baraban, O. Zhahlovska, S. Tsyrylnyk, A. Rudyk, Development and Research of Models and Processes of Formation in Silicon Plates p-n Junctions and Hidden Layers under the Influence of Ultrasonic Vibrations and Mechanical Stresses, *Key Engineering Materials* 844 (2020) 155–167. doi:10.4028/www.scientific.net/kem.844.155.
- [18] C. J. Evans, C. M. Nunn, S. W. L. Cheng, J. D. Franson, T. B. Pittman, Experimental storage of photonic polarization entanglement in a broadband loop-based quantum memory, *Physical Review A*, 108 (2023) L050601. doi:10.1103/physreva.108.l050601.
- [19] A.O. Semenov, S.V. Baraban, O.V. Osadchuk, O.O. Semenova, K.O. Koval, A.Yu. Savytskyi, Microelectronic Pyroelectric Measuring Transducers, In: Tiginyanu, I., Sontea, V., Railean, S. (Eds.) 4th International Conference on Nanotechnologies and Biomedical Engineering. ICNBME 2019. IFMBE Proceedings, vol. 77, 2019, pp. 393-397. doi:10.1007/978-3-030-31866-6\_72.
- [20] R. T. Prabu, M. L. Leon, P. Balasubramanian, S. H. Ahammad, Md. A. Hossain, A. N. Z. Rashed, Simulative study of high speed light modulated measured sources for high optical network transmission efficiency, *Journal of Optical Communications*, 0 (2023). doi:10.1515/joc-2023-0003.
- [21] M. M. A. Eid, A. E.-N. A. Mohammed, A. N. Z. Rashed, Simulative study on the cascaded stages of traveling wave semiconductor optical amplifiers based multiplexing schemes for fiber optic systems improvement, *Journal of Optical Communications*, 0 (2021). doi:10.1515/joc-2020-0281.
- [22] H. Tang et al., A Review of High-Power Semiconductor Optical Amplifiers in the 1550 nm Band, *Sensors* 23.17. (2023) 7326. doi:10.3390/s23177326.